



Tilting and Stick–Slip Tests for Evaluating Static and Dynamic Frictional Properties of Rock Discontinuities

Ömer Aydan¹ · Ryouji Kiyota² · Naoki Iwata² · Neamatullah Malistani¹

Received: 12 October 2019 / Accepted: 30 July 2023 / Published online: 30 August 2023
© The Author(s), under exclusive licence to Springer-Verlag GmbH Austria, part of Springer Nature 2023

Abstract

Static and dynamic frictional properties of rock discontinuities are of great importance in the evaluation of the initiation of failure and post-failure motions of rock engineering structures as well as the rupture and strong motions induced by earthquake faults in earthquake science. Nevertheless, experiments on static and dynamic frictional properties of rock discontinuities are very rare. In this study, the authors describe tilting and stick–slip experiments on various natural rock discontinuities and saw-cut surfaces to determine their static and dynamic frictional properties. Furthermore, these experimental results are compared with each other to discuss the static and dynamic frictional properties of rock discontinuities from tilting and stick–slip tests. Experimental results show that peak (static) friction angle for discontinuity surfaces obtained from tilting tests and stick–slip experiments are very close to each other.

Highlights

- In this paper, it is demonstrated that the static and dynamic frictional properties of rock discontinuities can be determined from tilting and stick–slip tests.
- Experimental results confirm that peak (static) friction angle for discontinuity surfaces obtained from tilting tests are very close to those obtained from stick–slip experiments.
- The experimental results could be useful for researchers dealing with the estimation of post-failure motions of failed bodies in Rock Mechanics and Rock Engineering as well as strong motion simulations in Earthquake Science and Engineering.

Keywords Discontinuities · Static · Dynamic · Kinetic · Friction angle · Tilting · Stick–Slip

1 Introduction

The static and dynamic friction angles of rock discontinuities such as joints, faults, and intrinsic discontinuities such as bedding planes, sheeting joints, flow planes and faults are quite important as they influence the initiation of failure and post-sliding conditions of natural and artificial rock structures as well as in earthquake science (Aydan 1989, 2017; Aydan et al. 1996, 2011). For example, the estimation of post-failure motions of natural or artificial rock slopes is of great importance.

Various techniques are used to measure the frictional properties of discontinuities and interfaces. Direct shear tests and triaxial testing could be used (e.g., Jaeger 1959; Ripley and Lee 1962; Byerlee 1970; Coulson 1971; Goodman and Ohnishi 1973; Barton 1973; Jaeger and Cook 1979; Aydan et al. 2004, 2016; Muralha et al. 2014). However, such tests require some high-capacity equipment and they are generally used to determine frictional characteristics under high normal loads. If cohesion or adhesion do not exist, a simple method of testing is the tilting (tilt table) test, whose principles can be found in many earlier textbooks in physics (e.g., Edwin and Bergen 1891, 2015; Dare and Slusher 1899, 1983; Meriam and Kraig 1951, 2012).

Stick–slip testing technique could be also utilized for evaluating frictional characteristics of rock discontinuities, and there are some reports on the stick–slip behavior of discontinuities (e.g., Brace and Byerlee 1966; Byerlee

✉ Ömer Aydan
aydan@tec.u-ryukyu.ac.jp

¹ Department of Civil Engineering, University of the Ryukyus,
1 Senbaru, Nishihara, Okinawa 903-0213, Japan

² Chuden Engineering Consultants, Hiroshima, Japan

1970, 1978). Ohta and Aydan (2010) are probably the pioneers to utilize this technique in the field of rock mechanics and rock engineering for evaluating the stick–slip behavior of rock discontinuities although some theoretical models were already available (Bowden and Leben 1939; Bowden and Tabor 1950; Jaeger and Cook 1979). However, there is no report on the application of this technique to infer frictional characteristics of rock discontinuities and compare them with other methods in the literature of rock mechanics and rock engineering, yet.

This study is concerned with the determination of the static and kinetic frictional properties of rock discontinuities from both tilting tests and stick–slip tests and compare the results with each other. The static and kinetic friction angles of rock discontinuities can be determined from tilting tests if the testing device is equipped with appropriate instruments such as non-contact laser transducers, accelerometers (e.g., Aydan 2016, 2022a; Aydan et al. 2017, 2020). The stick–slip testing device can also be used to measure frictional characteristics during the initiation and slip regime (e.g., Kiyota et al. 2018, 2019; Aydan et al. 2020; Aydan 2022a). The authors performed numerous tilting tests and stick–slip tests on the same rock discontinuities and evaluated the static and kinetic frictional characteristics of polished, saw-cut and natural discontinuities associated with various rocks.

The paper presents the outcomes of these experiments and examines the interrelations among the results of the tilting tests and stick–slip tests. The natural rock discontinuities include schistosity planes in quartzite, green-schist, cooling surfaces in andesite, tension joint from granite of Salang Pass; the saw-cut surfaces are from Ryukyu limestone, Motobu limestone, andesite and basalt of Mt. Fuji, dolomite of Kita-Daitojima, grano-diorite of Ishigaki and Inada granite; the polished surfaces are from gabbro and dolomite; the fault plane surface specimens with striations

are from the Efes Fault Zone in Western Turkey (Fig. 1) and it is a normal fault (Aydan et al. 2020, 2022).

2 Frictional Behavior of Discontinuities

The frictional properties of discontinuities and interfaces received great attention probably a thousand years ago since Sumerians, who established the fundamentals of science and engineering we use today (e.g., Kramer 1959, 1963; Dowson 1979; Frangipane 1997). However, the studies on frictional characteristics of rock discontinuities in modern days are quite recent (e.g., Jaeger 1959, 1971; Byerlee 1978; Goodman and Ohnishi 1973; Barton 1976). Bowden and Tabor (1950) in the field of mechanical engineering suggested that friction components of an interface consist of actual frictional resistance and the geometrical friction associated with morphology of the interface. This concept was also extended to rock discontinuities by considering a simple geometry of rock discontinuities by Patton (1966) and Goldstein et al. (1966) and the frictional resistance is assumed to consist of basic friction angle and additional friction angle resulting from the surface roughness, which is sometimes interpreted as dilation angle and corresponds to slope angle of a typical asperity (e.g., Bowden and Tabor 1950; Patton 1966). Barton and Choubey (1977) generalized this concept by assuming that the frictional resistance consists of the basic friction angle and joint roughness coefficient (JRC). Barton and Choubey (1977) suggested 10 roughness profiles with assigned JRC values. The basic friction angle and JRC are fundamentally obtained from a back analysis of the results of tilting (tilt table) test on discontinuities of the same rock having a saw-cut surface and natural surface. Alejano et al. (2018)

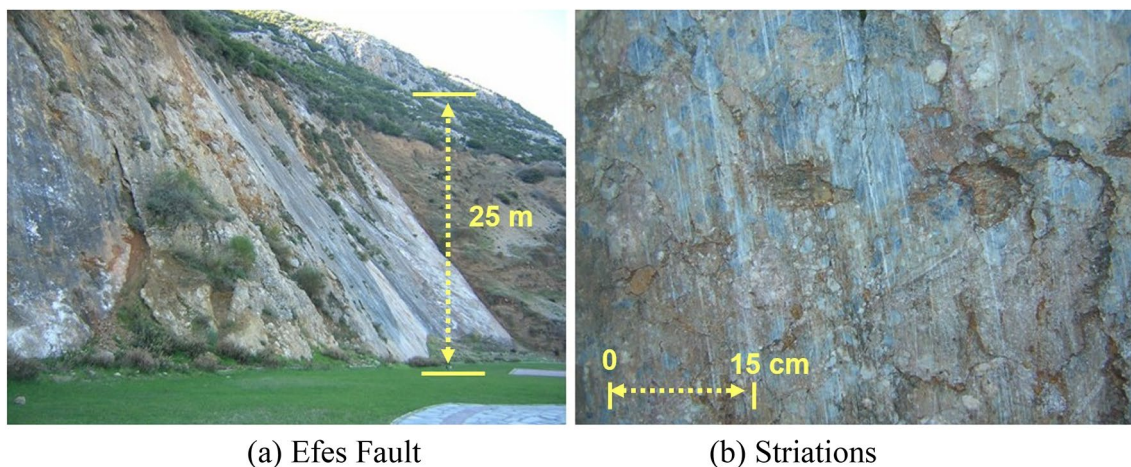


Fig. 1 A view of Efes Fault and a close-up view of its surface

developed an ISRM suggested method for obtaining the basic friction angle from tilting (tilt) tests.

Static and dynamic shearing tests on rock discontinuities are important for constitutive modeling under static and dynamic conditions (e.g., Aydan 2022a; Aydan et al. 1994, 1995, 1996, 2015, 2007, 2016; Ohta and Aydan 2010). When structures are constructed on/in rock masses having various kinds geological discontinuities, their stability and response during excavation or failure require the determination of the shearing characteristics of the discontinuities. Dynamic conditions may be particularly significant in relation to the long-term stability of the structures and during earthquakes as well as in the earthquake mechanism due to the rate dependency of shear strength (e.g., Dieterich 1972; Aydan et al. 1994, 2016, 2017; Aydan 2022a, b; Iwata et al. 2016, 2019).

3 Theory of Tilting Tests

Tilting (tilting table or tilt) tests are known as a laboratory technique for measuring the friction angle in physics and illustrating the concept of friction. This technique is one of the most popular techniques due to its simplicity, and it is one of the most suitable techniques to perform and to obtain the frictional characteristics of rock discontinuities (e.g., Carsey and Farrar 1976; Barton and Choubey 1977; Aydan et al. 1995, 2017; Alejano et al. 2018).

Let us assume that a block is put upon a base block with an inclination α as illustrated in Fig. 2. The dynamic force equilibrium equations for the block can be easily written as follows:

For the s -direction

$$W \sin \alpha - S = m \frac{d^2s}{dt^2} \tag{1}$$

For the n -direction

$$W \cos \alpha - N = m \frac{d^2n}{dt^2} \tag{2}$$

where W, N, S, m, s, n, t , and α are weight, normal force, shear force, mass, coordinate parallel to sliding direction, coordinate in normal direction, time and inclination of the basal plane, respectively. The mass of the block is related to its weight through the well-known relation, namely, $m = W/g$ where g is gravitational acceleration.

Let us further assume that the following frictional constitutive laws holds at the initiation and during the motion of the block (Aydan and Ulusay 2002; Aydan 2017) as illustrated in Fig. 3b:

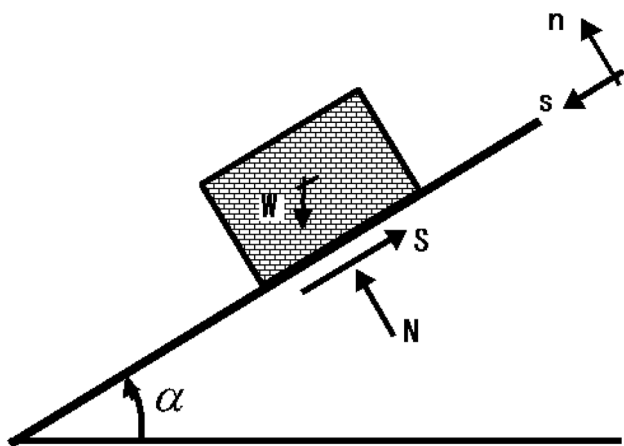
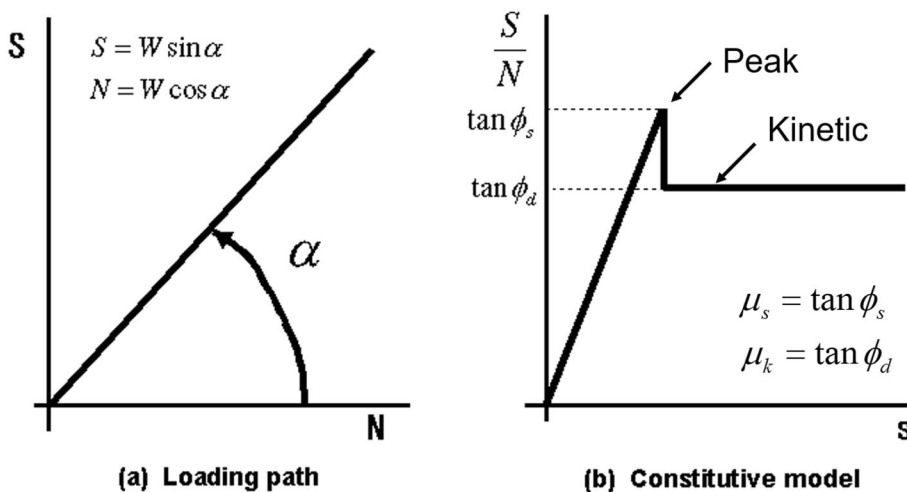


Fig. 2 Mechanical model for tilting experiments (α : inclination; W : block weight; S and N : Shear and Normal forces; s, n : shear and normal directions)

Fig. 3 Loading path in tilting experiments and constitutive relation (ϕ_s, ϕ_d : static and kinetic friction angles; μ_s, μ_d : static and kinetic friction coefficients)



At the initiation of sliding motion,

$$\frac{S}{N} = \tan \phi_s \quad (3)$$

During the sliding motion,

$$\frac{S}{N} = \tan \phi_d, \quad (4)$$

where ϕ_s and ϕ_d are static and kinetic friction angles.

At the initiation of sliding, the inertia terms are zero so that the following relation is obtained:

$$\tan \alpha = \tan \phi_s. \quad (5)$$

The above relation implies that the angle of inclination at the initiation of sliding should correspond to the static friction angle of the discontinuity.

If the inertia term for normal direction is negligible during the motion and if the frictional resistance is assumed to be reduced to kinetic friction instantaneously, one obtains the following relations for the motion of the block

$$\frac{d^2s}{dt^2} = A, \quad (6)$$

where $A = g(\sin \alpha - \cos \alpha \tan \phi_d)$ and g is gravitational acceleration.

The integration of differential Eq. (6) yields the following

$$s = A \frac{t^2}{2} + C_1 t + C_2, \quad (7)$$

where C_1 and C_2 are integration coefficients. As the following conditions hold at the initiation of sliding.

$$s = 0 \text{ and } v = 0 \text{ at } t = T_s, \quad (8)$$

where v and T_s are velocity and time of sliding initiation. Equation (7) takes the following form

$$s = \frac{A}{2} (t - T_s)^2. \quad (9)$$

Coefficient A can be obtained either from a given displacement s_n at a given time t_n with the condition,

$$A = 2 \frac{s_n}{(t_n - T_s)^2} \text{ for } t_n > T_s, \quad (10)$$

or from the application of the least square technique to measured displacement response as follows (see Appendix for details)

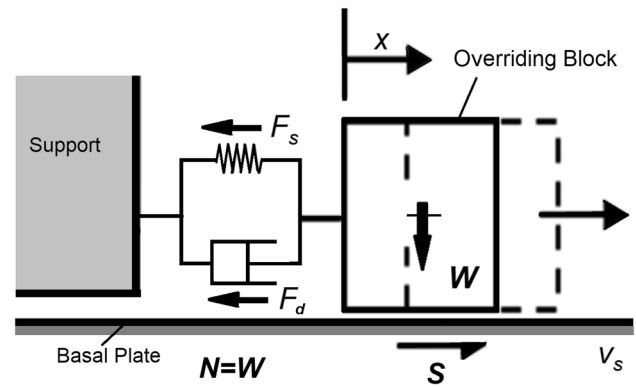


Fig. 4 Mechanical modeling of stick–slip phenomenon. v_s : the velocity of moving base; k : the stiffness of the system; η : viscous resistance coefficient; W : the block weight; S : shear resistance; F_s and F_d are elastic reaction and viscous resistance,

$$A = 2 \frac{\sum_{i=1}^n s_i (t_i - T_s)^2}{\sum_{i=1}^n (t_i - T_s)^4}. \quad (11)$$

Once the constant A is determined, the dynamic friction angle is obtained from the following relation

$$\phi_d = \tan^{-1} \left(\tan \alpha - \frac{1}{\cos \alpha} \cdot \frac{A}{g} \right). \quad (12)$$

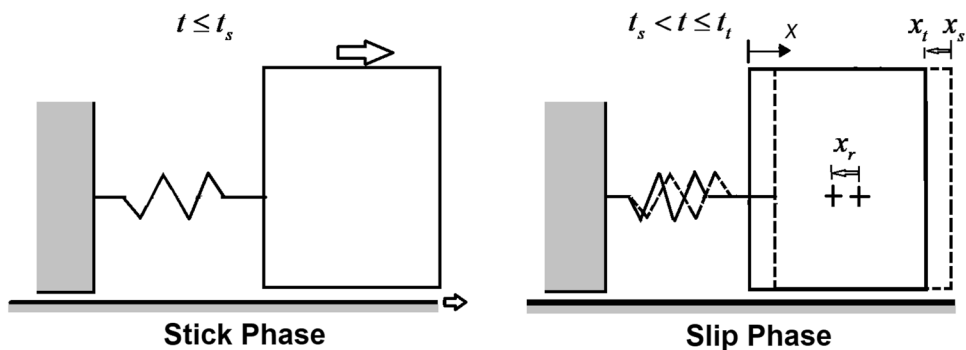
4 Theory of Stick–Slip Tests

In this model, the basal plate is assumed to be moving with a constant velocity v_s , and overriding block is assumed to be elastically supported by the surrounding medium as illustrated in Fig. 4. However, if damping exists, the support may be assumed as visco-elastic. The basic modeling concept assumes that the relative motion occurs between the basal plate and overriding block and it involves the stick and slip phases of the overriding block as illustrated in Fig. 5a. Let us assume that the motion of the overriding block on the basal plate moving with a constant velocity can be modeled as stick–slip phenomenon (e.g., Bowden and Leben 1939; Bowden and Tabor 1950; Jaeger & Cook 1979; Ohta and Aydan 2010; Aydan 2017, 2022a). The derivation of the governing equations of the motion of the overriding block shown in Fig. 4 are described as given below.

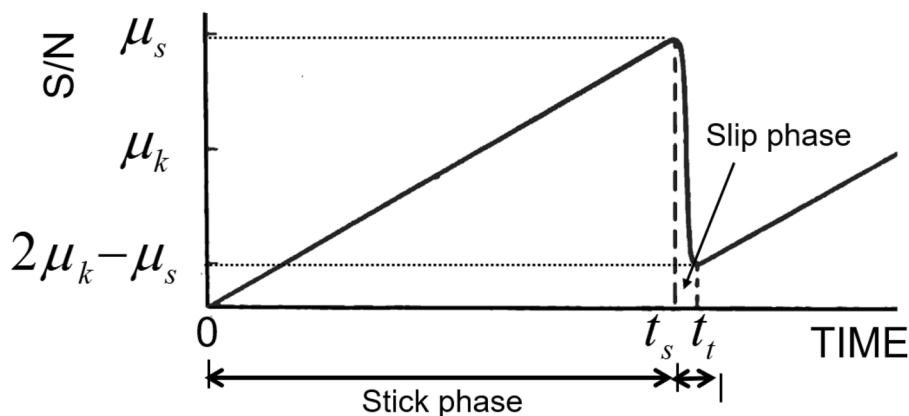
During the stick phase, the following holds

$$\dot{x} = v_s, \quad F_s = k \cdot x, \quad (13)$$

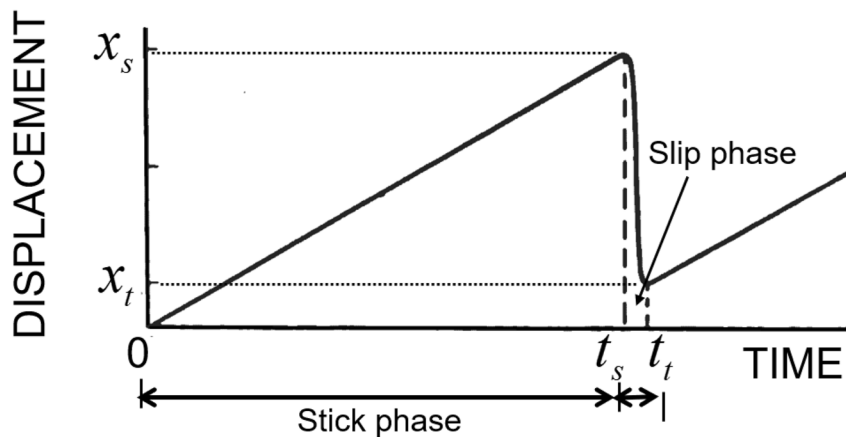
Fig. 5 Frictional forces during a stick-slip cycle. μ_s, μ_k : static and kinetic friction coefficients; t_s, t_t : time at the initiation (x_s) and termination (x_t) of slip,



(a) Schematic illustration of typical stick and slip phases. x_r : the amount of slip



(b) Variation of frictional resistance during a typical stick-slip cycle



(c) Variation of relative slip during a typical stick-slip cycle

where v_s is the velocity of the moving base plate and k is the stiffness of the system. The initiation of slip obeys the friction law as given below (see Fig. 3b):

$$S = \mu_s N, \tag{14}$$

where μ_s is static friction coefficient, N is normal force. For the block shown in Fig. 4, the normal force is equal to the

block weight W and it is related to the mass m and gravitational acceleration g through mg . It is assumed that the frictional resistance (S/N) is assumed to be reduced from the static friction coefficient (μ_s) to the kinetic friction coefficient (μ_k) as illustrated in Fig. 3b. During slip phase, the forces are kinetic friction, elastic restoring force (proportional to displacement x), viscous resistance (proportional

to velocity \dot{x}), and inertia components and the force equilibrium takes the following form (Fig. 4):

$$-kx - \eta\dot{x} + \mu_k W = m \frac{d^2x}{dt^2}, \quad (15a)$$

where μ_k is the dynamic friction coefficient and η is the viscous resistance coefficient. If viscous resistance is assumed to be negligible, Eq. (15a) takes the following form

$$-kx + \mu_k W = m \frac{d^2x}{dt^2}. \quad (15b)$$

The solution of the ordinary differential equation above can be obtained as.

$$x = A_1 \cos \Omega t + A_2 \sin \Omega t + \mu_k \frac{W}{k}. \quad (16)$$

Figure 5 shows a schematic illustration of a stick–slip cycle and variation of associated parameters. If the initial conditions ($t = t_s$, $x = x_s$ and $\dot{x} = v_s$) are introduced into Eq. (16), the integration constants A_1 and A_2 are obtained as follows (Figs. 4, 5).

$$\begin{aligned} x &= \frac{W}{k} (\mu_s - \mu_k) \cos \Omega(t - t_s) + \frac{v_s}{\Omega} \sin \Omega(t - t_s) + \mu_k \frac{W}{k} \\ \dot{x} &= -\frac{W}{k} (\mu_s - \mu_k) \Omega \sin \Omega(t - t_s) + v_s \cos \Omega(t - t_s) \\ \ddot{x} &= -\frac{W}{k} (\mu_s - \mu_k) \Omega^2 \cos \Omega(t - t_s) - v_s \Omega \sin \Omega(t - t_s), \end{aligned} \quad (17)$$

where $\Omega = \sqrt{k/m}$ and $x_s = \mu_s \frac{W}{k}$.

At $t = t_t$ the slip terminates and the velocity of the overriding block becomes equal to the velocity of the moving basal plate, which is given as $\dot{x} = v_s$. This yields the period of slip as (see Fig. 5b, c) for the illustrations of initiation and termination of a typical stick–slip cycle):

$$t_t = \frac{2}{\Omega} \left(\pi - \tan^{-1} \left(\frac{(\mu_s - \mu_k) W \Omega}{k \cdot v_s} \right) \right) + t_s, \quad (18)$$

where $x_s = v_s \cdot t_s$, which is illustrated in Fig. 5b, c. The rise time, which corresponds to the slip period, is given by

$$t_r = t_t - t_s. \quad (19)$$

The rise time can be specifically obtained from Eq. 19 by inserting the slip period t_t given by Eq. 18 as

$$t_r = \frac{2}{\Omega} \left(\pi - \tan^{-1} \left(\frac{(\mu_s - \mu_k) W \Omega}{k \cdot v_s} \right) \right). \quad (20)$$

If the velocity of the moving basal plate is negligible, that is, $v_s \approx 0$, the rise time (t_r) from Eq. (20) reduces to the following form

$$t_r = \pi \sqrt{\frac{m}{k}}. \quad (21)$$

Thus, the amount of slip is obtained through the utilization of Eqs. (19) and (21) as

$$x_r = |x_t - x_s| = 2 \frac{W}{k} (\mu_s - \mu_k). \quad (22)$$

The force drop during slip is obtained from Eq. (22) as

$$F_d = 2(\mu_s - \mu_k) W. \quad (23)$$

Static and kinetic friction angles from a typical slip phase shown in Fig. 5b, c can be determined from Eq. (23). Re-arranging Eq. (23) yields the following relation for kinetic friction angle as

$$\phi_k = \tan^{-1} \left(\mu_s - \frac{1}{2} \frac{F_d}{N} \right). \quad (24)$$

As noted from (Eq. 22), the increase of the normal load on the blocks increases the amount of slip, decreases the velocity during slip (Eq. 17) and prolongs the period of stick–slip cycles as noted from Eq. 20 or 21.

5 Device for Tilting and Stick–Slip Tests

The device used for both tilting and stick–slip tests is the same and it is capable of performing different tests. In other words, it is a multi-purpose experimental device (Aydan 2017, 2022a). Figure 6 illustrates the main components of the device. The endless belt part of the device is capable of performing a classical base-friction model test and this function allows us to carry out stick–slip experiments with the utilization of load cell, laser displacement transducers, acoustic emission sensors and accelerometers and the

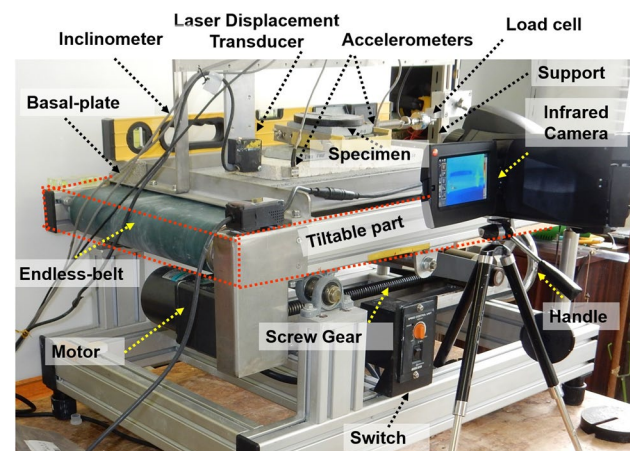


Fig. 6 An overall view of the device and its main components

data acquisition equipment as explained in the following subsections.

The device can also be used to measure the surface morphology of discontinuities along a given line. In other words, it is possible to measure digital surface profiles using two laser transducers (one for profile and one for block velocity) (see Aydan 2020, p. 31) and various surface morphology parameters of rock discontinuities can be evaluated (e.g., Myers 1962; Aydan and Shimizu 1995; Aydan et al. 1996).

The endless part forms also tiltable base and it can be inclined up to 90 degrees. Tilting tests can be carried out together with the utilization of laser displacement transducers, acoustic emission sensors and accelerometers and the data acquisition equipment. While simple tilting tests described in the ISRM SM (Alejano et al. 2018; Aydan et al. 1995, 1996) can be easily carried out by the device by using only an inclinometer, the laser transducers particularly allow us to measure not only peak friction angle but also kinetic friction angle (Aydan 2017, 2022a; Aydan et al. 2017). The accelerometers can also be used to measure the inclination as well as to assess the initiation of slip and its response during the entire slip process.

5.1 Device for Tilting Tests

The experimental device consists of a table (endless belt part) tilted manually through a screw gear connected to a wheel. During the experiments, the displacement of the block and inclination of the table are measured through laser displacement transducers produced by KEYENCE and OMRON while the acceleration responses parallel and perpendicular to the shear movement are measured by a

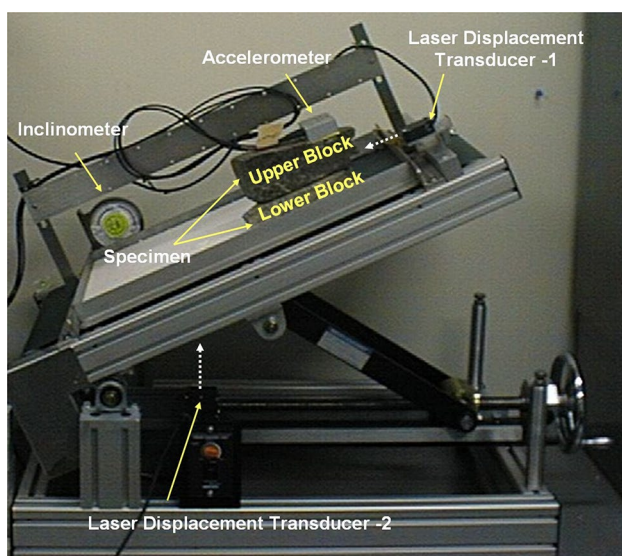


Fig. 7 A view of a typical experimental set-up for tilting tests

three component accelerometer (TOKYO SOKKI) attached to the upper block and the WE7000 (YOKOGAWA) data acquisition system. The measured displacement and accelerations are recorded onto lap-top computers. The weight of the accelerometer is about 98 gf. Figure 7 shows the experimental set-up.

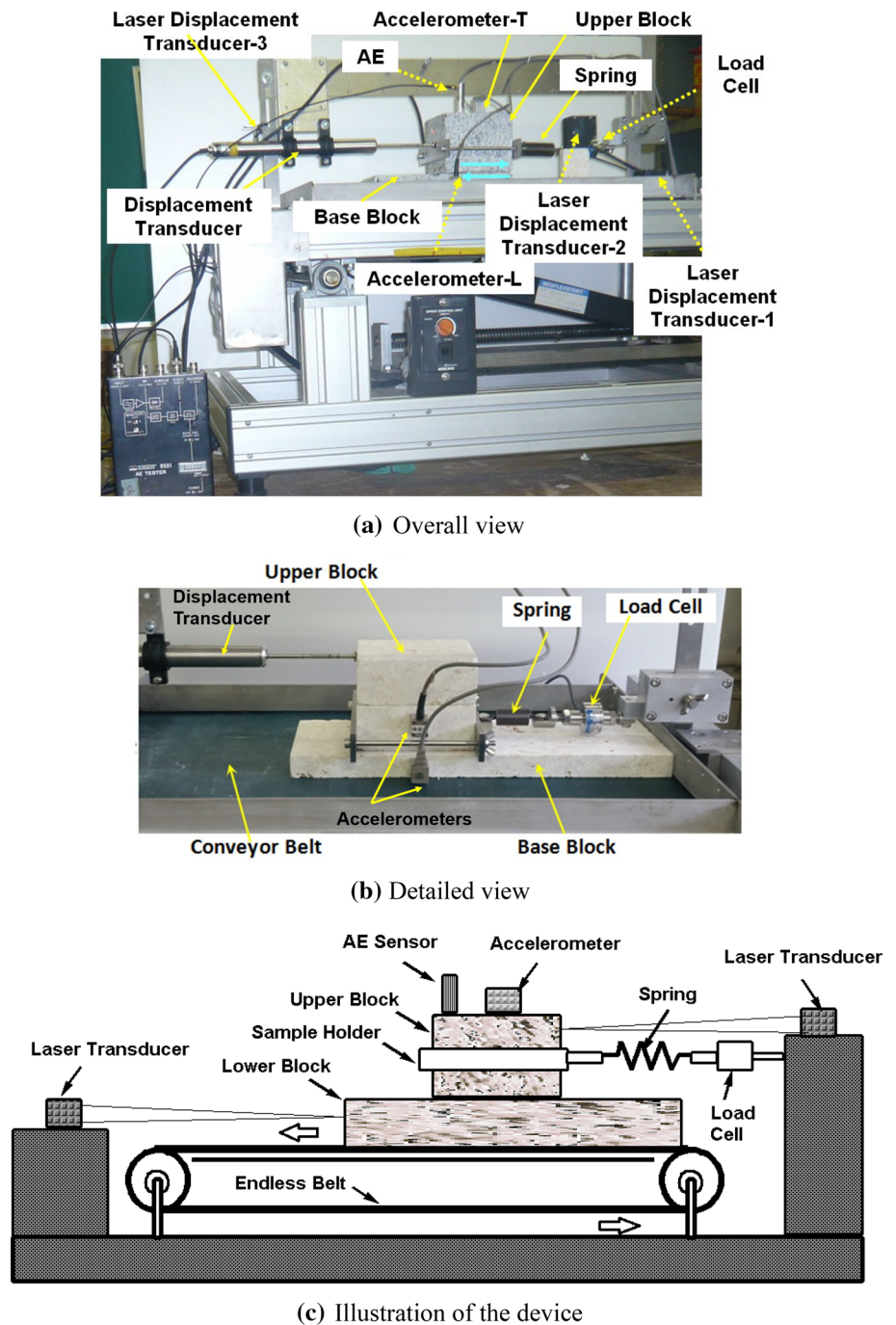
5.2 Device for Stick–Slip Tests

Figure 8 shows a view of the experimental set-up for stick–slip experiments described by Aydan (e.g., Aydan et al. 2011; Ohta and Aydan 2010; Aydan and Ohta 2011). The experimental device consists of an endless conveyor belt and a fixed frame, and it is schematically illustrated in Fig. 8c. The inclination of the conveyor belt can be varied so that various tangential and normal gravitational forces can be easily imposed on the specimen as desired. The base can be tilted for tilting tests as shown in Fig. 7. To study the actual frictional resistance of interfaces of rock blocks, the lower block is attached to the belt while the upper block is attached to the fixed frame through a spring as illustrated in Figs. 6 and 8. We conducted experiments using rock specimens with planes having different surface morphologies. The base blocks were 200–400 mm long, 100–150 mm wide and 40–100 mm thick. The upper block was 100–200 mm long, 100 mm wide and 150–200 mm high.

To measure the frictional force acting on the upper block, the load cell (KYOWA LUR-A-200NSA1) is installed between the spring and the fixed frame as seen in Figs. 6 and 8. During experiments, the displacement of the block is measured through the laser displacement transducers described in the previous section, and a contact type displacement transducer with a measuring range of 70 mm, while the acceleration responses parallel and perpendicular to the belt movement are measured by the same three-component accelerometer attached to the upper block. The measured displacement, acceleration and force are recorded onto laptop computers through the WE7000 (YOKOGAWA) data acquisition system.

When the upper block moves together on the base block at a constant velocity (stick phase, which is similar to static situation), the spring is stretched at a constant velocity. The shear force increases to some critical value and then a sudden slip occurs with an associated spring force drop. Because the unstable sliding of the upper block occurs periodically, the upper block slips violently over the base block. Figure 9 shows displacement–friction coefficient responses (S: Shear force; N: Normal force) of the Efes fault specimen denoted BFP1-TFP1 under three different normal loads (850 gf, 1580 gf, 2580 gf). The normal loads on the specimens can be easily increased in the experiments. The frictional force drop is $2(\mu_s - \mu_k)W$ and it is given by Eq. 23, in which μ_s and μ_k are the static and kinetic (or dynamic) friction

Fig. 8 Experimental set-up for stick–slip tests



coefficients, respectively. As noted from Fig. 9, the measured responses are in accordance with those expected from theoretical estimations presented in Sect. 4. As the stiffness of the spring remains constant, the stress drop is more sudden under low normal stress compared to that under high normal stress as anticipated from Eq. (22). This fact may also have some implications in earthquake mechanics and associated strong motions in relation to the variability of the stiffness of Earth's crust from region to region (e.g., Aydan 2022a). Furthermore, if the static friction coefficient is equal to the

kinetic friction coefficient, the stress drop would be nil and this would correspond to creeping faults.

6 Experimental Results

In this section, the experimental results on frictional characteristics of discontinuities obtained from stick–slip tests and tilting tests are presented and discussed. Although the stick–slip tests and tilting tests may seem to be different,

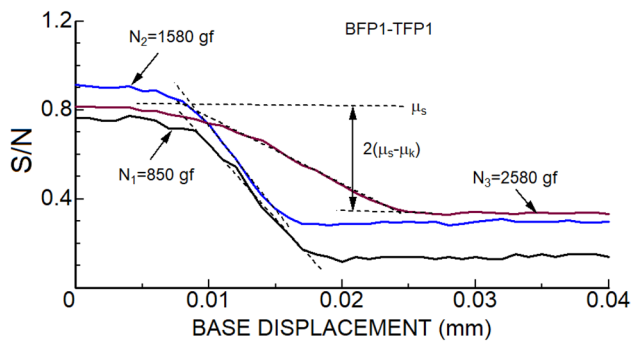


Fig. 9 Responses during a typical slip phase under three different normal loads (N_1, N_2, N_3). μ_s, μ_k : static and kinetic friction coefficients; S and N: Shear and Normal forces

it should be noted that a stick-slip cycle is quite similar to a tilting test as stick phase (zero relative velocity) corresponds to the static situation during tilting before the commencement of the slip. The slip phase in the stick-slip tests is a dynamic process and this phase is fundamentally equivalent to the slip phase in tilting tests. Furthermore, it may be appropriate to say that a stick-slip test allows one to test the frictional characteristics of the same surface repeatedly while a tilting test would correspond to single testing situation.

6.1 Discontinuities

Discontinuities used in the tilting and stick-slip experiments are listed in Table 1. Rocks involve igneous, metamorphic

Table 2 Determined static and dynamic friction angle of discontinuities from stick-slip tests on samples of the Efes fault

Test No	N (gf)	Static (°)	Dynamic (°)
Efesfault_bfp1_tfp1_t1	850	37.6, 37.6	34.4, 24.3
Efesfault_bfp1_tfp1_t2	1580	42.0, 42.0, 35.0	30.7, 35.4, 27.9
Efesfault_bfp1_tfp1_t3	2580	39.4, 28.4	30.1, 26.8

bfp1 base block fault plane, *tfp1* top block fault plane, *t1, t2, t3* test number

and sedimentary rocks sampled from Japan, Afghanistan, China and Turkey. The discontinuities involve cooling joints, schistosity planes, bedding planes, fault surfaces and saw-cut surfaces with or without polishing. Furthermore, fault surfaces have striations and experiments on such specimens are carried out parallel and perpendicular to the striations. In Table 1, the basic friction angle of discontinuities are also given so that the roughness of tested discontinuities can be inferred (see Tables 2 and 3).

6.2 Tilting Tests

A series of tilting tests are carried out on the discontinuities listed in Table 1. Base inclination, relative slip responses recorded in all experiments and time-slip responses are fitted to the function given by Eq. (9) to obtain both the static and kinetic (or dynamic) friction angles. It should be noted that the slip is restrained after a certain amount of relative slip in all experiments. The measured time-slip responses during a tilting test on a rough discontinuity plane of granite

Table 1 A list of localities, type and basic friction angle of discontinuities and unit weight of host rocks

Rock	Locality	Country	Type	UW (kN/m ³)	ϕ_b (°)
Andesite	Mt. Fuji	Japan	Saw-cut	26.1	24.9
Andesite	Mt. Aso	Japan	Cooling	26.6	26.1
Basalt	Mt. Fuji	Japan	Saw-cut	24.1	23.0
Quartzite	Bayındır	Türkiye	Schistosity	25.1	26.1
Quartzite	Kumamoto	Japan	Schistosity	27.7	28.5
Diorite	Ishigaki	Japan	Saw-cut	26.5	29.2
Gabro	Unknown	China	Saw-cut-P	29.8	23.7
Limestone	Ryukyu	Japan	Saw-cut	22.9	27.7
Limestone	Motobu	Japan	Saw-cut	25.3	25.3
Dolomite	Kita-Daitojima	Japan	Saw-cut-P	26.2	22.0
Granite	Inada	Japan	Rough	25.3	25.3
Granite	Inada	Japan	Saw-cut	25.3	25.3
Granite	Salang	Afghanistan	Saw-cut	25.9	30.1
Marl-BP	Babadag	Türkiye	Bedding	19.0	32.0
Marl-BP	Babadag	Türkiye	Saw-cut	19.0	28.2
Limestone	Efes Fault	Türkiye	Fault plane	26.0	30.6
Limestone	Efes Fault	Türkiye	Saw-cut	26.0	24.9

P polished, *UW* unit weight; ϕ_b basic friction angle

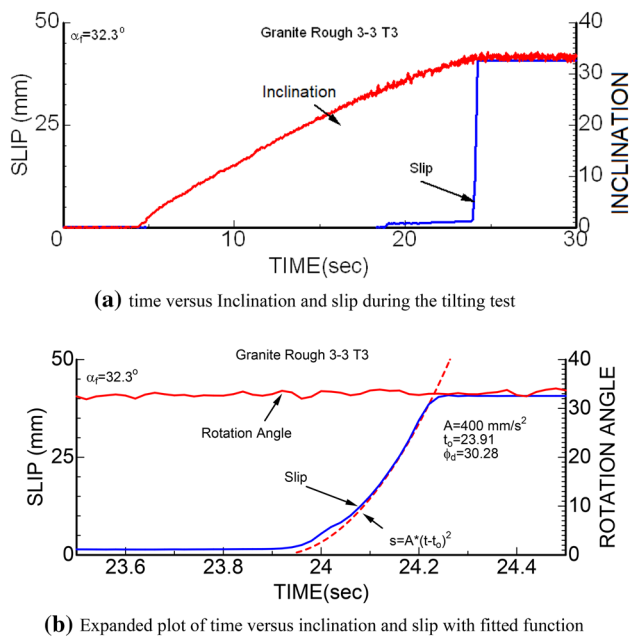


Fig. 10 Displacement response of rough discontinuity of granite during a tilting test and a fitted function to slip response (α_s : tilt angle; t_0 : slip initiation time; t : time; g : gravitational acceleration; ϕ_d : kinetic (dynamic) friction angle; A : constant)

are shown in Fig. 10 as an example. Figure 10a shows the time-inclination and related time-slip response during the experiment while Fig. 10b shows close-up plots of time-inclination angle and related time-slip response for the period between 23.5 and 24.5 s. In this particular experiment, the relative movement of the upper block is allowed to be 40 mm. Figure 10b also shows the fitted function to time-slip response and its coefficient. The fitted function is fairly consistent with experimental results for a given time interval and the kinetic friction angle of the discontinuity was obtained as 30.28 while the static friction was 32.3°. Figure 10 shows views of the tilting test on rough discontinuity plane of granite.

The static and dynamic (kinetic) friction coefficients of the rough interface of granite were calculated from measured

displacement response and weight of upper block using the tilting testing equipment shown in Fig. 11. Utilizing Eq. (12) and value of A of the fitted function, the static and kinetic friction angles were estimated to be within a range of 32.3°–37.6° and 30.3°–35.6°, respectively. The tests were repeated three times and the ranges correspond to the tests results obtained from three tests with a great caution to clean up the interface after each test according to the ISRM Suggested Method (Alejano et al. 2018).

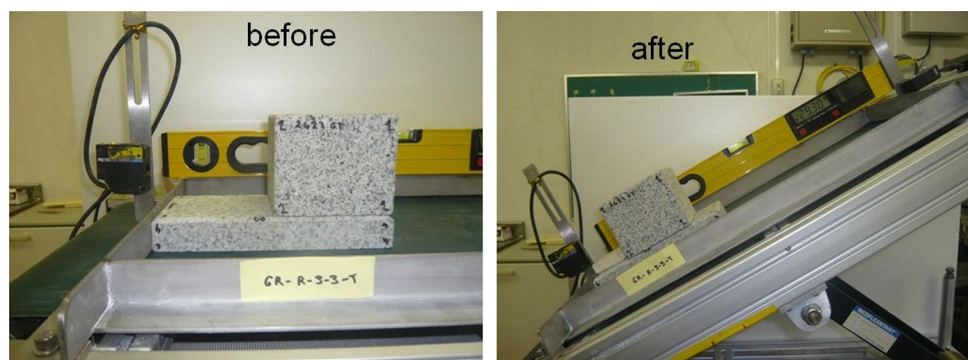
Similarly, the experimental results on saw-cut discontinuity surfaces of Ryukyu limestone specimens are plotted in Fig. 12, which shows time-inclination and related time-slip responses measured during a tilting experiment on a saw-cut surface of Ryukyu limestone. Figure 12b shows close-up plots of time-inclination angle and related time-slip response for the period between 12.8 and 13.6 s. Utilizing Eq. (12) and value of A of the fitted function, the static and kinetic friction angles of the saw-cut surfaces were calculated from measured time-slip response as explained in the previous section and they were estimated to be within a range of 28.8°–29.6° and 24.3°–29.2°, respectively. Similarly, the ranges are the results of three experiments performed with a great caution to clean up Ryukyu limestone saw-cut discontinuity planes after each test according to the ISRM Suggested Method (Alejano et al. 2018).

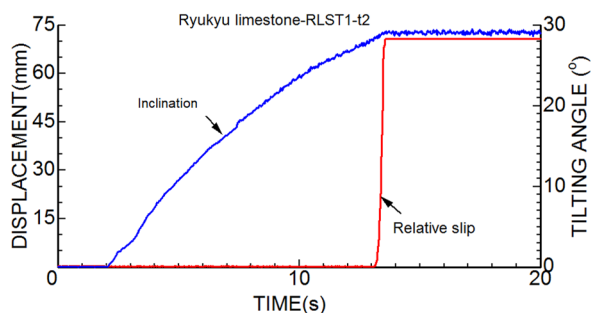
Figure 13a shows an example of time-inclination, acceleration and slip records during a tilting experiment on a specimen having fault surfaces from the Efes Fault shown in Fig. 1. The slip induced a fluctuation of acceleration in the direction of slippage. The high acceleration is due to shock caused by the top block when it hit the barrier to terminate its motion.

The inclination angle is directly obtained from the acceleration component in the slip direction. The procedure described in Sect. 3 was applied to the slip response of the fault surface specimen between 26.073 and 26.5 s as shown in Fig. 13b. The static and kinetic friction angles were obtained as 33° and 29.5° in this particular test.

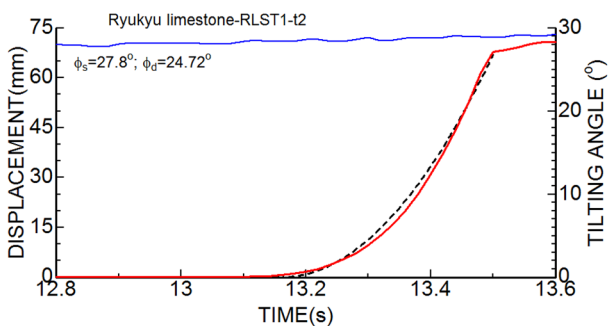
Experiments were carried out by considering the orientation of striation on the fault surface. Friction angles of

Fig. 11 Views of tilting experiment on rough discontinuity plane of granite



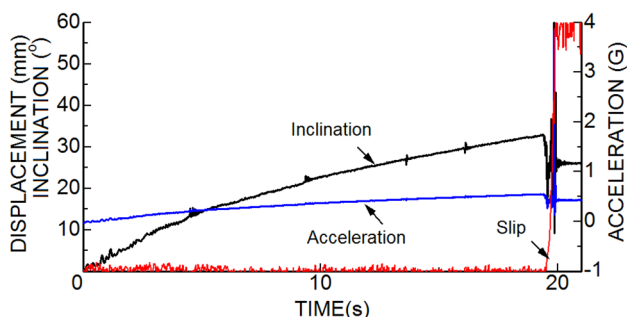


(a) Time versus inclination and slip during the tilting test

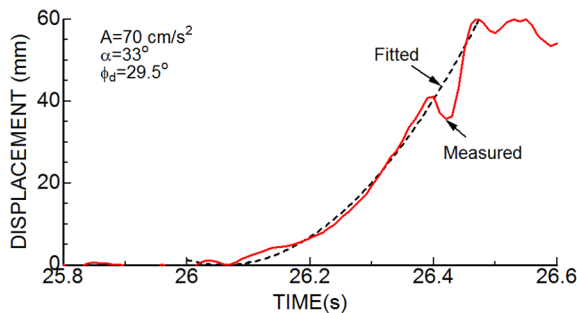


(b) Expanded plot of time versus inclination and slip with fitted function

Fig. 12 Time versus inclination and slip records of tilting experiment on a saw-cut discontinuity plane of Ryukyu limestone specimen during a tilting test (ϕ_s , ϕ_d : static and kinetic (dynamic) friction angles)



(a) Plots of time versus inclination, acceleration and slip during a tilting experiment.



(b) Determination of dynamic (kinetic) friction angle

Fig. 13 a Measured responses and b determination of dynamic friction angle of a fault plane specimen from Efes fault zone from the measured slip response and fitted function

the fault surface parallel and perpendicular to the direction of striations are given in Table 3. The friction angle was smaller when testing was carried out parallel to the striation direction while it was higher when the experiments were carried out perpendicular to the striation direction. These results are consistent with previous experimental results reported by Aydan et al. (1996) and indicate the frictional anisotropy of the natural discontinuities.

6.3 Stick-Slip Experiments

A series of stick-slip experiments are carried out on the discontinuities listed in Table 1 using the stick-slip device shown in Fig. 8. Stick-slip tests are carried out on the same specimens used in tilting experiments presented in previous section after cleaning the surface of fault plane specimens according to the ISRM Suggested Method on tilting experiments (Alejano et al. 2018). Responses of frictional resistance and acceleration in some of these experiments are reported herein. The duration of stick-slip experiments is much longer than that in tilting experiments. As the relative slip history involves many cycles of slip, the surface conditions are likely to be influenced by the slip history. In other words, some gouge-like material may accumulate on the discontinuity surface and this may influence the overall frictional resistance during the many cycles of slip. Therefore, the evaluations are limited to the first two cycles of stick-slip phases.

The peak (static) friction angle can be evaluated from the S/N response while the kinetic friction angle can be obtained from the theoretical relation (24). Figures 14 and 15 show the measured stick-slip responses of discontinuity surfaces of granite and Ryukyu limestone specimens, respectively. Peak (static) friction angle for both discontinuity surfaces obtained from tilting tests (37.6°) and stick-slip experiments (36.1° – 37.4°) are very close to each other when the results given in Table 3 are taken into account. The residual or kinetic (dynamic) friction angles for rough discontinuity surface of granite are also very close to each other. It was 35.9° in tilting tests while it ranged between 34.6° and 35.0° in the stick-slip tests.

Similarly, the kinetic friction angle (24.6° – 26.8°) of the saw-cut discontinuity surface of the Ryukyu limestone, that was obtained from stick-slip experiments, was very close to that (24.7°) obtained from tilting experiments. Nevertheless, the kinetic (dynamic) friction angle obtained from stick-slip tests is generally lower than those obtained from the tilting experiments.

Experiments were carried out on fault surface specimens from the Efes Fault (see Fig. 1) under three different normal loads, namely dead-weight (850 gf), 1580 gf and 2580 gf. Figure 16 shows the base displacement-frictional resistance responses in initial stages of the stick-slip experiment

Table 3 Static and kinetic friction of discontinuities tested under tilting and stick–slip testing conditions

Rock	Locality	Tilting		Stick–slip	
		Static	Kinetic	Static	Kinetic
Andesite	Mt. Fuji	24.9	23.3	24.1	21.3
Andesite	Mt. Aso	36.6	34.6	34.6	32.4
Basalt	Mt. Fuji	23.0	21.9	22.5	20.3
Quartzite	Bayındır	38.3	32.0	37.9	29.4
Quartzite	Kumamoto	36.9	34.1	37.1	30.4
Diorite	Ishigaki	33.4	28.9	32.1	28.7
Gabro	Unknown (polished)	23.7	21.7	22.5	19.5
Limestone	Ryukyu	27.7	24.7	28.5–31.1	24.6–26.8
Limestone	Motobu	31.2	28.7	33.4	28.3
Dolomite	Kita-Daitojima (polished)	22.0	19.8	23.3	15.6
Granite	Inada (rough)	37.6	35.9	36.1–37.4	34.6–35.0
Granite	Inada	35.8	33.6	36.1	32.0
Granite	Inada (saw-cut)	27.0	24.9	25.3	20.0
Granite	Salang	43.2	37.2	41.6	35.8
Marl-BP	Babadag	40.5	38.7	40.3	31.9
Marl-BP	Babadag	34.7	31.9	35.0	27.3
Limestone	Efes Fault-FS (parallel to striation)	30.6	26.4	30.6	26.4
Limestone	Efes Fault-FS (perpendicular to striation)	36.7	32.3	35.2	32.2
Limestone	Efes Fault (saw-cut)	24.9	23.2	25.0	21.8

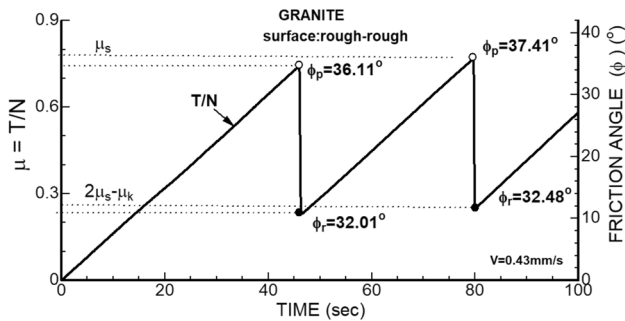


Fig. 14 Stick–slip response of rough discontinuity plane of granite (μ_s , μ_k : static and kinetic friction coefficients; S and N: Shear and Normal forces)

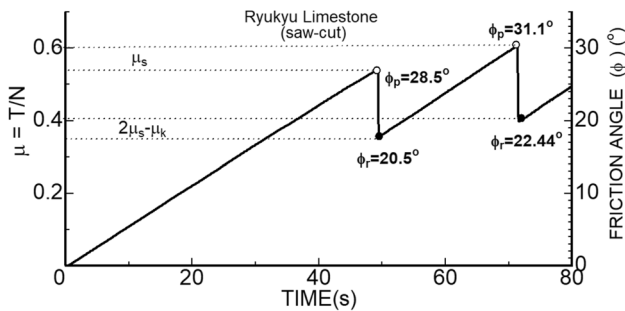


Fig. 15 Stick–slip response of saw-cut plane of Ryukyu limestone (μ_s , μ_k : static and kinetic friction coefficients; S and N: Shear and Normal forces)

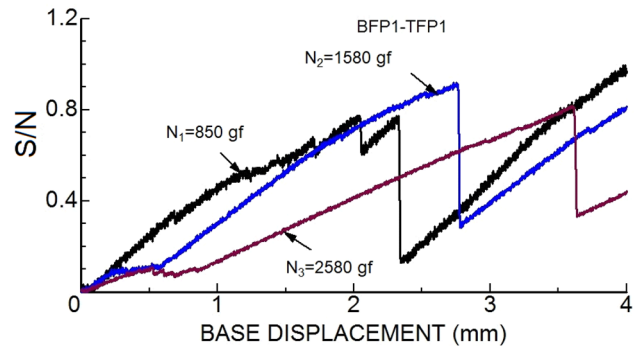


Fig. 16 Relative base displacement and frictional resistance responses in initial stages of the stick–slip experiment on a fault plane specimen from Efes Fault zone under three different normal loads (N_1 , N_2 , N_3); S and N: Shear and Normal forces

under three different normal loads. Table 2 gives the static and kinetic (dynamic) friction angles obtained from the responses shown in Fig. 16.

The static friction angle from stick–slip tests perpendicular to the striation ranged between 37.7° and 42° while it was 36.7° from tilting tests. For the same specimen, the dynamic (kinetic) friction angle ranged between 27.9° and 35.0° (see Table 2), it was 32.3° for tilting experiments. Despite some scattering, the results obtained from the two testing techniques are quite similar to each other.

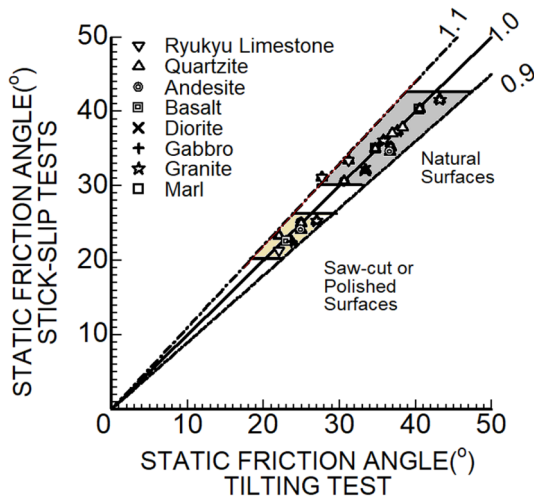


Fig. 17 Comparison of static friction angles obtained from tilting and stick-slip experiments

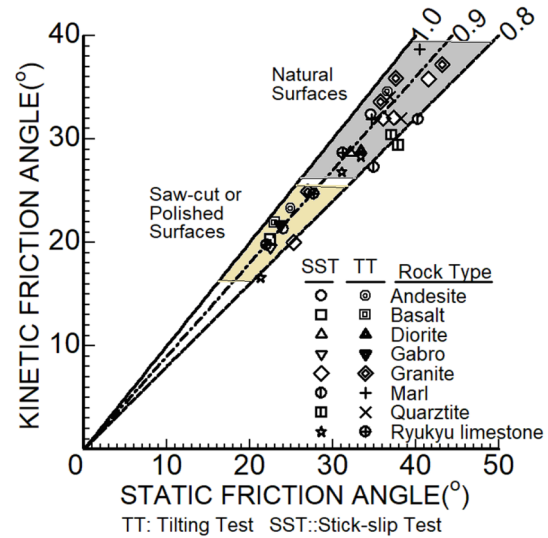


Fig. 19 Comparison of static and kinetic friction angles obtained from tilting experiments on all rock specimens (limestone) (ϕ_s ; ϕ_d : static and kinetic (dynamic) friction angle)

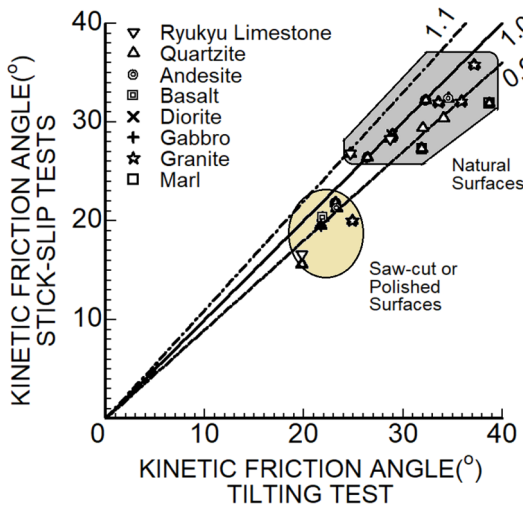


Fig. 18 Comparison of kinetic friction angles obtained from tilting and stick-slip experiments

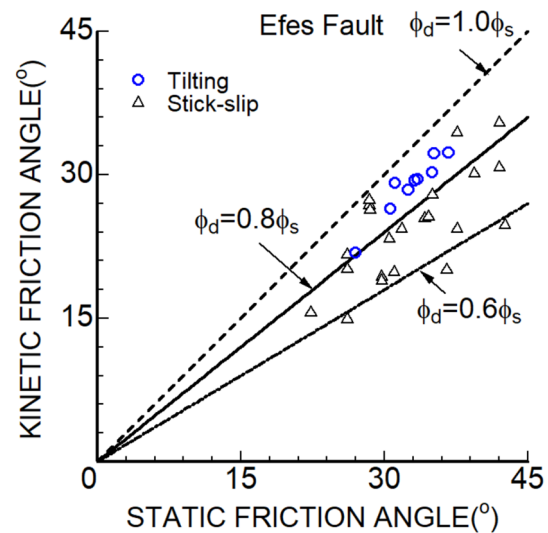


Fig. 20 Comparison of static and kinetic friction angles obtained from tilting experiments on Efes fault specimens (limestone) (ϕ_s ; ϕ_d : static and kinetic (dynamic) friction angle)

7 Comparisons and Discussions

In this section, the experimental results on frictional properties obtained from tilting tests and stick-slip experiments are compared with each other. Furthermore, the possibility of obtaining both peak (static) and kinetic (dynamic) friction angles from any of these experimental techniques is discussed.

First the static (peak) friction angles determined from tilting tests are compared with those obtained from stick-slip experiments. Figure 17 shows the plots of static friction angle from tilting tests versus static friction angle from stick

slip tests with the consideration of rock type. In the plots, the results for saw-cut and polished surfaces are differentiated from those of natural surfaces. The results are close to the line with a gradient 1, which implies that the static friction angles obtained from tilting and stick slip experiments are almost the same irrespective of rock and discontinuity type.

The kinetic (dynamic) friction angle of discontinuity surfaces obtained from the stick-slip experiments and tilting experiments are plotted in Fig. 18 by considering rock type as well as the surface conditions of tested samples.

As noted in Fig. 18, they are close to the line with a gradient 1. Nevertheless, the kinetic (dynamic) friction angle obtained from stick–slip tests is slightly lower than those obtained from the tilting experiments.

Figure 19 shows the plots of static friction angle versus kinetic friction angle obtained from tilting tests and stick–slip tests. The results are plotted with different symbols for each rock type as well as testing technique. As noted from the figure, the ratio of kinetic friction angle over the static friction angle is generally less than 1.0 and greater than 0.8. This finding is in agreement with the previous experimental results reported by Aydan et al. (2017).

The experimental results obtained in the tests on the Efes Fault specimens (brecciated limestone) are plotted for static versus dynamic friction angle in Fig. 20 by distinguishing the results of tilting and stick–slip tests. Compared to the experimental results in Fig. 19, the ratio of kinetic friction angle over the static friction angle is generally less than 1.0 and greater than 0.6. The results are somewhat different in regard with the lower bound compared to Fig. 19. This might be due to some inherent characteristics of fault plane specimens resulting from the past relative large displacement greater than 25 m for this normal fault. Although some differences are noted between the friction angles of the fault surface and other discontinuities, the overall trend is quite similar.

In accordance with the previously reported results by Aydan et al. (2017), it is interesting to note that the kinetic friction angles of various rock discontinuities except fault planes are about 0.8–0.9 times that of the static friction angles irrespective of discontinuity type.

8 Conclusions

In this study, the authors described an experimental study on various natural rock discontinuities, fault surfaces and artificially prepared saw-cut surfaces utilizing tilting and stick–slip experiments to determine their static and dynamic frictional properties and to show that static and dynamic frictional properties can be obtained from these two experimental techniques.

Experimental results indicated that the peak (static) friction angles of discontinuity surfaces obtained from tilting tests and stick–slip experiments are very close to each other. Nevertheless, the kinetic (dynamic) angles obtained from the stick–slip experiments are slightly lower than those obtained from the tilting experiments.

In accordance with the previously reported results by Aydan et al. (2017), it is interesting to note that the ratio of kinetic friction angle to static friction angle of discontinuities surfaces is less than 1.0 and greater than 0.8. However, the ratio of kinetic friction angle to static friction angle of fault surfaces can be as low as 0.6.

Appendix: Derivation of Eq. (11)

As shown in Sect. 3.1, the relative slip response of the sliding block during the slip-phase can be given by the following relation

$$S = \frac{A}{2} (t - T_s)^2. \quad (25)$$

As pointed out in the same subsection, coefficient A can be obtained from a given displacement s_n at a given time t_n . However, there are many observation data and the application of the least square technique to measured displacement response become necessary. The residual between the measured response and fitted function is given as

$$r_i = s_i - S(t_i, A). \quad (26)$$

The sum of squared residual is written as

$$E = \sum_{i=1}^n r_i^2, \quad (27a)$$

or

$$E = \sum_{i=1}^n (s_i - S(t_i, A))^2. \quad (27b)$$

Minimizing the error function (E) with respect to coefficient A and requiring the gradient to be zero as given below

$$\frac{\partial E}{\partial A} = \frac{\partial}{\partial A} \left(\sum_{i=1}^n (s_i - S(t_i, A))^2 \right) = 0, \quad (28)$$

results in

$$\sum_{i=1}^n s_i (t_i - T_s)^2 - \sum_{i=1}^n \frac{A}{2} (t_i - T_s)^4 = 0. \quad (29)$$

Re-arranging the equation above yields the following, which is given by Eq. (11)

$$A = 2 \frac{\sum_{i=1}^n s_i (t_i - T_s)^2}{\sum_{i=1}^n (t_i - T_s)^4} \quad (30)$$

Declarations

Conflict of Interest The authors declare that they have no conflict of interest.

References

- Alejano L, Muralha J, Ulusay R, Li, C, Pérez-Rey I, Karakul H, Chrysanthakis P, Aydan Ö (2018) ISRM suggested method for determining the basic friction angle of planar rock surfaces by means of tilt tests. *Rock Mech Rock Eng* 51(12):3853–3859
- Aydan Ö 1989 The stabilisation of rock engineering structures by rock-bolts. Doctorate Thesis, Nagoya University
- Aydan Ö (2016) Considerations on friction angles of planar rock surfaces with different surface morphologies from tilting and direct shear tests 6p, Bali, on CD, Paper No.57
- Aydan Ö (2017) *Rock dynamics*. CRC Press, Taylor and Francis Group, p 462 (ISRM Book Series No. 3, ISBN 9781138032286)
- Aydan Ö (2020) *Rock mechanics and rock engineering: volume 1-fundamentals of rock mechanics* (p.31). CRC Press, Taylor and Francis Group, p 379
- Aydan Ö (2022a) *Earthquake science and engineering*. CRC Press, Taylor and Francis Group, p 496 (ISBN 9780367758776)
- Aydan Ö (2022b) Physics, motions and prediction of earthquakes from rock mechanics perspective. In: Li et al (eds) *RocDyn4, Rock dynamics: progress and prospect*, vol 1. CRC Press, pp 3–15
- Aydan Ö, Shimizu Y (1995) Surface morphology characteristics of rock discontinuities with particular reference to their genesis. *Fractography*, Geological Society Special Publication No. 92, pp 11–26
- Aydan Ö, Ohta Y (2011) The erratic pattern screening (EPS) method for estimation of co-seismic deformation of ground from acceleration records and its applications. In: *Seventh National Conference on Earthquake Engineering*, Istanbul, Turkey, Paper No 66: pp 1–10
- Aydan Ö, Ulusay R (2002) Back analysis of a seismically induced highway embankment during the 1999 Düzce earthquake. *Environ Geol* 42:621–631
- Aydan Ö, Akagi T, Okuda H, Kawamoto T (1994) The cyclic shear behaviour of interfaces of rock anchors and its effect on the long term behaviour of rock anchors. *Int. Symp. on New Developments in Rock Mechanics and Rock Engineering*, Shenyang, pp 15–22
- Aydan Ö, Shimizu Y, Kawamoto T (1995) A portable system for in-situ characterization of surface morphology and frictional properties of rock discontinuities. *Field measurements in geomechanics*. In: 4th International Symposium, pp 463–470
- Aydan Ö, Shimizu Y, Kawamoto T (1996) The anisotropy of surface morphology and shear strength characteristics of rock discontinuities and its evaluation. In: *NARMS'96*, pp 1391–1398
- Aydan Ö, Ulusay R, Kumsar H (2004) The inference of possible focal plane solutions of active faults from their striations and their relations to actual focal plane solutions. In: *Proceedings of the 5th International Symposium on Eastern Mediterranean Geology (5th ISEMG)*, Thessaloniki, Greece, pp 821–824
- Aydan Ö, Daido M, Tokashiki N, Bilgin A, Kawamoto T (2007) Acceleration response of rocks during fracturing and its implications in earthquake engineering. 11th ISRM Congress, Lisbon, vol 2, pp 1095–1100
- Aydan Ö, Ohta Y, Daido M, Kumsar H, Genis M, Tokashiki N, Ito T, Amini M (2011) Chapter 15: Earthquakes as a rock dynamic problem and their effects on rock engineering structures. In: Zhou Y, Zhao J (eds) *Advances in rock dynamics and applications*. CRC Press, Taylor and Francis Group, pp 341–422
- Aydan Ö, Fuse T, Ito T (2015) An experimental study on thermal response of rock discontinuities during cyclic shearing by Infrared (IR) thermography. In: *Proc. 43rd Symposium on Rock Mechanics*, JSCE, pp 123–128.
- Aydan Ö, Tokashiki N, Tomiyama J, Iwata N, Adachi K, Takahashi Y (2016) The development of a servo-control testing machine for dynamic shear testing of rock discontinuities and soft rocks. In: *EUROCK2016, Ürgüp*, pp 791–796
- Aydan Ö, Tokashiki N, Iwata N, Takahashi Y, Adachi K (2017) Determination of static and dynamic friction angles of rock discontinuities from tilting tests. In: *14th Domestic Rock Mechanics Symposium of Japan, Kobe*, Paper No. 041, p 6 (in Japanese)
- Aydan Ö, Kiyota R, Iwata N, Kumsar H, Sakamoto I (2020) An experimental study on frictional properties of faults. In: *47th Japan Rock Mechanics Symposium*, JSCE, Tokyo, pp 197–202
- Aydan Ö, Kumsar H, Iwata N (2022) Characterization and properties of faults zones and their effect on stress changes during earthquake. *RocDyn4, Xuzhou*
- Barton M (1973) Review of a new shear strength criterion for rock joints. *Eng Geol* 7:287–332
- Barton N (1976) The shear strength of rock and rock joints. *Int J Rock Mech Min Sci* 13:255–279
- Barton NR, Choubey V (1977) The shear strength of rock joints in theory and practice. *Rock Mech* 12(1):1–54
- Bowden FP, Leben L (1939) The nature of sliding and the analysis of friction. *Proc R Soc Lond A* 169:371–391
- Bowden FP, Tabor D (1950) *The friction and lubrication of solids*. The Clarendon Press, Oxford
- Brace WF, Byerlee JD (1966) Stick-slip as a mechanism for earthquakes. *Science* 153:990–992
- Byerlee JB (1970) The mechanics of stick-slip. *Tectonophysics* 9(1970):475–486
- Byerlee JD (1978) Friction of rocks. *Pure Appl Geophys* 116:615–626
- Carsey DC, Farrar NS (1976) A simple sliding apparatus for the measurement of rock joint friction. *Geotechnique* 26(2):382–386
- Coulson JH (1971) Shear strength of flat surfaces in rock. In: *Proceedings of the 13th Symposium on rock mechanics*, Illinois. ASCE 1971, pp 77–105
- Dare A, Slusher H (1899) *Schaum's outline of theory and problems of physics for engineering and science*. McGraw-Hill, p 359
- Dare A, Slusher H (1983) *Schaum's outline of theory and problems of physics for engineering and science*. McGraw-Hill, p 359
- Dieterich JH (1972) Time dependent friction in rock. *J Geophys Res* 77:3690–3697
- Dowson D (1979) *History of tribology*. Longman, London
- Edwin HH, Bergen JY (1891, 2015) *A textbook of physics, largely experimental*. H. Holt and Company, New York, p 596
- Frangipane MA (1997) 4th millennium temple palace complex at Arslantepe-Malatya. North-South relations and the formation of early state societies in the northern regions of greater Mesopotamia. *Paleorient* 23(1):45–73
- Goodman RE, Ohnishi Y (1973) Undrained shear tests on jointed rock. *Rock Mech* 5:129–149
- Goldstein M, Goosev B, Pyrogovsky N, Tulinov R, Turovskaya A (1966) Investigation of mechanical properties of cracked rock. In: *1st ISRM Congress*, Lisbon, 1, 521–524
- Iwata N, Adachi K, Takahashi Y, Aydan Ö, Tokashiki N, Miura F (2016) In: *Fault rupture simulation of the 2014 Kamishiro Fault Nagano Prefecture Earthquake using 2D and 3D-FEM*. *EUROCK2016, Ürgüp*, pp 803–808
- Iwata N, Kiyota R, Aydan Ö, Ito T, Miura F (2019) Effects of fault geometry and subsurface structure model on the strong motion and surface rupture induced by the 2014 Kamishiro Fault Nagano Earthquake. In: Aydan Ö, Ito T, Seiki T, Kamemura K, Iwata N (eds) *Proceedings of 2019 Rock Dynamics Summit in Okinawa*, 7–11 May, 2019, Okinawa, Japan, ISRM, pp 222–228
- Jaeger JC (1959) *Frictional Properties of Joints in Rocks*. *Geofisica Pura Et Applicata* 43:148–158
- Jaeger JC (1971) Friction of rocks and stability of rock slopes. *Geotechnique* 21:97–134
- Jaeger JC, Cook NWG (1979) *Fundamentals of rock mechanics*, 3rd edn. Chapman and Hall, London

- Kiyota R, Iwata N, Takahashi Y, Adachi K, Aydan Ö (2018) Stick-slip behavior of rock discontinuities and its implications on the simulation of earthquake rupturing. In: The 3rd Int. Symp on Rock Dynamics, RocDyn3, Trondheim, CRC Press, pp 563–568
- Kiyota R, Iwata N, Aydan Ö, N Tokashiki (2019) Experimental study of scale effect in rock discontinuities on stick-slip behavior. In: Aydan Ö, Ito T, Seiki T, Kamemura K, Iwata N (eds) Proceedings of 2019 Rock Dynamics Summit in Okinawa, 7–11 May, 2019, Okinawa, Japan, ISRM, pp 119–123
- Kramer SN (1959) *History begins at sumer: thirty-nine firsts in man's recorded history*. University of Pennsylvania Press
- Kramer SN (1963) *Sumerians: their history, culture and character*. The University of Chicago Press, Chicago, p 355p
- Meriam JL, Kraig LG (1951) *Engineering mechanics, statistics*, 7th edn. Wiley
- Meriam JL, Kraig LG (2012) *Engineering mechanics, statistics*, 7th edn. Wiley, Berlin
- Muralha J, Grasselli G, Tatone B, Blumel M, Chryssantankis P, Jiang Y (2014) ISRM suggested method for laboratory determination of the shear strength of rock joints: revised version. *Rock Mech Rock Eng* 47(1):291–302
- Myers NO (1962) Characterization of surface roughness. *Wear* 5(3):182–189
- Ohta Y, Aydan Ö (2010) The dynamic responses of geomaterials during fracturing and slippage. *Rock Mech Rock Eng* 43(6):727–740
- Patton FD (1966) Multiple modes of shear failure in Rock. In: First International Conference on Rock Mechanics, Lisbon, Vol. 1, 509–513
- Ripley CF, Lee KL (1962) Sliding friction tests on sedimentary rock specimens. In: Trans. 7th Int. Congr. Large Dams. Rome, Vol. 4, 657–671

Publisher's Note Springer Nature remains neutral with regard to jurisdictional claims in published maps and institutional affiliations.

Springer Nature or its licensor (e.g. a society or other partner) holds exclusive rights to this article under a publishing agreement with the author(s) or other rightsholder(s); author self-archiving of the accepted manuscript version of this article is solely governed by the terms of such publishing agreement and applicable law.